Table of Results	Controls	EMCI	LMCI	AD
N with HBSI	113	106	96	36
HBSI left+right, ml/year	0.05 (0.11)	0.06 (0.10)	0.11(0.13)	0.19 (0.15)
MMSE score, /30	29 (1)	28 (2)	27 (2)	23 (2)
Age, years	74 (6)	70 (7)	72 (8)	75 (8)
% Male	50	58	50	69
WMH, ml median (IQR)	1.9 (3.5)	1.9 (4.5)	1.8 (3.9)	3.8 (8.1)
Log_2WMH	0.9 (1.9)	0.9 (1.9)	0.9 (1.9)	1.8 (2.0)
% CMB category*: 0, 1, 2-4, >4 CMBs	78,19,2,1	82,10,8,1	90,5,3,2	64,22,8,6
% Lacunes: 0, 1, 2 lacunes	97,3,0	94,5,1	98,2,0	97,0,3
Associations of log_2WMH with HBSI	**0.02 (0.00, 0.03) p = 0.008**	**0.01 (0.00, 0.02) p = 0.02**	**0.02 (0.01, 0.04) p = 0.002**	0.01 (-0.02, 0.03) p=0.6
Associations of CMB category with HBSI	**0 vs. 1 CMB: 0.07 (0.01, 0.12), p = 0.02** 0 vs. 2-4 CMBs: 0.06 (-0.10, 0.21), p=0.5 0 vs. >4 CMBs: 0.20 (-0.02, 0.43) p=0.08 **Overall test: P = 0.04**	0 vs. 1 CMB: 0.03 (-0.04, 0.09), p=0.4 0 vs. 2-4 CMBs: -0.02 (-0.09, 0.06), p=0.7 0 vs. >4 CMBs: -0.08 (-0.28, 0.12), p=0.4 Overall test: p=0.6	0 vs. 1 CMB: 0.09 (-0.04, 0.21), p=0.2 0 vs. 2-4 CMBs: 0.05 (-0.11, 0.22), p=0.5 0 vs. >4 CMBs: 0.09 (-0.10, 0.29), p=0.4 Overall test: p=0.4	**0 vs. 1 CMB: 0.14 (0.02, 0.26), p = 0.02** 0 vs. 2-4 CMBs: 0.02 (-0.17, 0.20), p=0.9 0 vs. >4 CMBs: 0.04 (-0.18, 0.27), p=0.7 Overall test: p=0.1
Associations of number of lacunes with HBSI	0 vs. 1 lacune: -0.04 (-0.17, 0.09) p=0.5	0 vs. 1 lacune: 0.04 (-0.05, 0.14), p= 0.3 0 vs. 2 lacunes: 0.12 (-0.08, -0.32) p=0.2 Overall test: P= 0.3	0 vs. 1 lacune: -0.10 (-0.29, 0.10), p=0.3	0 vs. 2 lacunes: 0.03 (-0.28, 0.34), p=0.8
Significant or trend-level independent associations with HBSI	**log_2WMH: 0.01 (0.00, 0.02) p = 0.03** **0 vs. 1 CMB: 0.06, (0.01, 0.12) p = 0.03**	log_2WMH: 0.01 (-0.00, 0.02) P=0.09	**log_2WMH: 0.02 (0.01, 0.04) p = 0.009**	**0 vs. 1 CMB: 0.15 (0.02, 0.27), p = 0.02**

Results are reported as mean (SD) unless otherwise indicated and for associations these are beta, (95% CI) and p value. Betas represent a one unit increase in the predictor variable on the outcome (mls / year loss hippocampal volume). * data missing in 3 controls, 2 EMCI. Bold indicates significant at p<0.05.

P4-525

DATA-DRIVEN TAU-PET COVARIANCE NETWORKS ENHANCE PREDICTION OF RETROSPECTIVE COGNITIVE CHANGE IN ALZHEIMER'S DISEASE

Jacob W. Vogel[1], Niklas Mattsson[2,3], Yasser Iturria Medina[1], Olof Strandberg[2], Michael Schöll[2,4], Christian Dansereau[5,6], Sylvia Villeneuve[7], Wiesje M. van der Flier[8], Philip Scheltens[8], Pierre Bellec[5,6], Alan C. Evans[1], Oskar Hansson[2,3], Rik Ossenkoppele[8], *[1]Montreal Neurological Institute, McGill University, Montreal, QC, Canada; [2]Clinical Memory Research Unit, Lund University, Lund, Sweden; [3]Memory Clinic, Skåne University Hospital, Lund, Sweden; [4]Wallenberg Centre for Molecular and Translational Medicine and the Department of Psychiatry and Neurochemistry, University of Gothenburg, Gothenburg, Sweden; [5]Department of Computer Science and Operations Research, Université de Montréal, Montreal, QC, Canada; [6]Centre de Recherche de l'Institut Universitaire de Gériatrie de Montréal, University of Montreal, Montreal, QC, Canada; [7]Department of Psychiatry, McGill University, Montreal, QC, Canada; [8]Alzheimer Center and Department of Neurology, VU University Medical Center, Amsterdam Neuroscience, Amsterdam, Netherlands. Contact e-mail: jacobwvogel@gmail.com*

Background: Positron emission tomography (PET) studies investigating filamentous tau pathology *in vivo* have used theory-derived regions-of-interest (ROIs) based on post-mortem studies. However, hypothesis-free data-driven approaches may yield ROIs optimized specifically for tau-PET data, resulting in better clinical utility. **Methods:** Demographic information, MMSE scores, AV1451-PET images and T1-weighted magnetic resonance images closest to PET were downloaded from the ADNI LONI website for 90 individuals (43 controls, 37 MCI, 10 AD dementia). AV1451 images were coregistered to each subject's T1 image and intensity normalized to the cerebellar gray matter. Images were then spatially normalized to the MNI152 template, stacked into a 4D image and masked with a liberal cortical mask including subcortical regions. This image stack was entered into a previously validated voxelwise clustering algorithm, which includes a procedure for defining optimal clustering solutions. The algorithm produces ROIs that represent patterns of AV1451 signal covariance across subjects. Linear mixed models were run assessing relationships between AV1451 signal within these ROIs and retrospective change in MMSE scores (575 observations). Corrected Aikake's information criterion (AICc) was used to compare models using our data-derived ROIs to models using theory-derived ROIs from three tau-PET studies published in 2016. All models were adjusted for age, gender and education. **Results:** The clustering algorithm identified a six-cluster solution to be the best solution (Figure 1). These clusters included a medial/inferior temporal ROI, a temporo-parietal predominant ROI, a frontal ROI, a dorsal ROI, a "partial-volume" ROI encircling the cortex, and an "off-target" ROI encompassing the subcortex, medial occipital lobe and the hippocampus. Across all ROIs tested, the model using the data-driven temporo-parietal ROI to predict retrospective change in MMSE (Figure 2) showed the best model fit (AICc=2312.56). With the exception of the stage IV ROI from Cho et al. (AICc=2320.54), no other ROIs demonstrated competitive model fit (ΔAICc > 10; Figure 3). **Conclusions:** Our clustering approach yielded a data-driven temporo-parietal ROI that is known to be highly AD specific and was identified as the best predictor of retrospective cognitive decline. The results suggest that hypothesis-free data-derived ROIs may offer enhanced predictive utility compared to theory-driven ROIs by utilizing information specific to tau-PET signal.

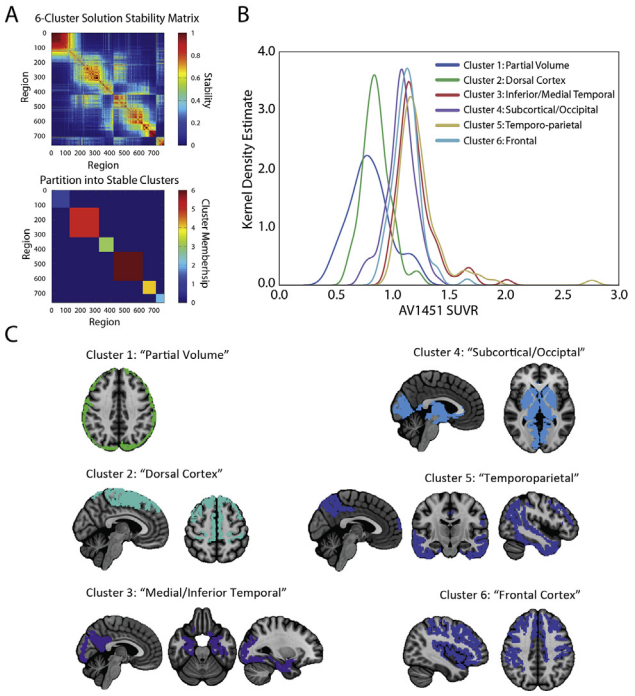

Figure 1. Six-cluster solution of tau-PET covariance networks. A. Voxel-wise images underwent dimension reduction with a region-growing algorithm for computation purposes. These small regions (atoms) were entered into a clustering analysis (Bootstrapping Analysis of Stable Clusters, Bellec et al., 2010, Neuroimage), which identified six clusters. The top image shows a stability matrix comparing the stability clustering between each atom and every other atom, organized by cluster membership. The bottom image shows the cluster partitioning. B. Kernel density estimate plots showcasing the distribution of AV1451 SUVR across subjects within each cluster. C. The six clusters identified by the clustering algorithm. SUVR = Standard uptake value ratio.

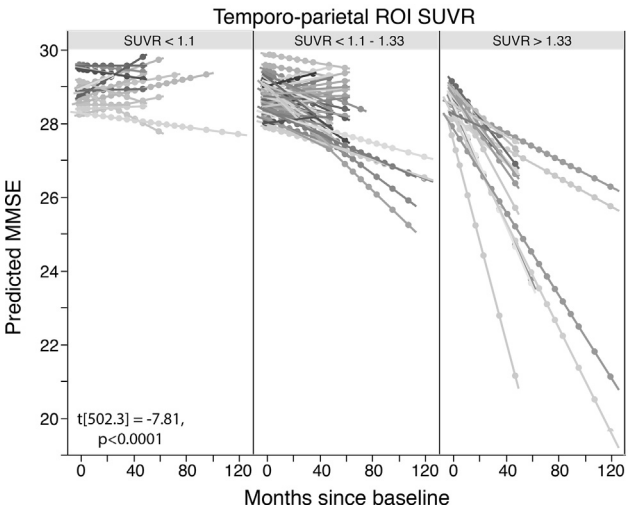

Figure 2. Effect of AV1451 standard uptake value ratio (SUVR) within the data-driven temporo-parietal ROI on retrospective longitudinal change in MMSE scores. From left to right, the three SUVR groups represent the lowest quintile, middle three quintiles, and highest quintile of AV1451 SUVR in the temporo-parietal ROI. Statistics in the bottom-right corner refer to the adjusted Temporo-parietal SUVR × Time interaction on MMSE.

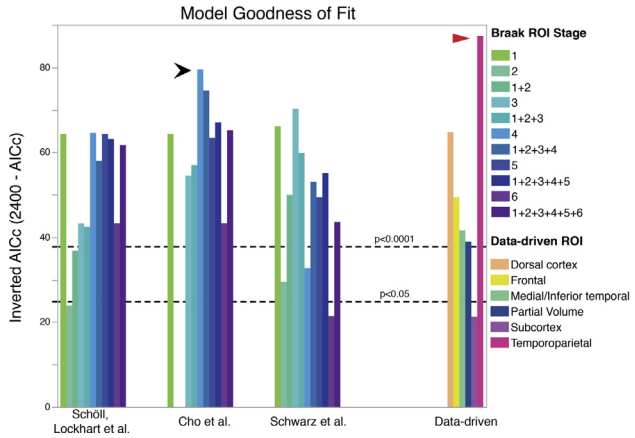

Figure 3. Linear mixed models comparing AVI451 signal to retrospective change in MMSE were run, controlling for age, sex and education. For each model, a different AVI451 ROI was used. ROIs included the six clusters identified in our analysis, as well as Braak stage ROIs taken from three different papers: Schöll, Lockhart et al., 2016 Neuron; Cho et al., 2016 Ann. Neurol.; Schwarz et al., 2016 Brain. Two versions of each Braak ROIs were created, one using regions from that stage only (e.g. Stage 3), and one combining all regions from that stage with all regions from previous stages (e.g. Stage 1+2+3). The fit of each model was measured using AICc; AICc was inverted for the graph so that higher value corresponds to better model fit. ΔAICc indicates differences in model fit, such that ΔAICc>10 suggests one model can be rejected in favor of the other. The data-driven temporoparietal ROI (red arrow) demonstrated the best model fit, and was superior to all other models except for the Braak Stage 4 ROI from Cho et al. (black arrow). Dotted lines indicate models where the ROI SUVR × Time interaction parameter within the model exceeds the given alpha level.

P4-526

HARMONIZATION OF NEUROIMAGING BIORMARKERS FOR NEURODEGENERATIVE DISEASES: A SURVEY FOR BEST PRACTICE GUIDELINES

Jorge Jovicich[1], Frederik Barkhof[2,3], Claudio Babiloni[4], Karl Herholz[5], Christoph Mulert[6], Bart N. M. van Berckel[7], Giovanni B. Frisoni[8,9], the SRA-NED JPND Working Group, *[1]University of Trento, Trento, Italy; [2]Amsterdam Neuroscience, VU University Medical Center, Amsterdam, Netherlands; [3]Translational Imaging Group, Centre for Medical Image Computing, University College London, London, United Kingdom; [4]Sapienza University of Rome, Rome, Italy; [5]University of Manchester, Manchester, United Kingdom; [6]Psychiatry and Psychotherapy University Medical Center Hamburg-Eppendorf, Hamburg, Germany; [7]VU University Medical Center, Amsterdam, Netherlands; [8]Lab Alzheimer's Neuroimaging & Epidemiology, IRCCS Fatebenefratelli, Brescia, Italy; [9]Memory Clinic and LANVIE - Laboratory of Neuroimaging of Aging, University Hospitals and University of Geneva, Geneva, Switzerland. Contact e-mail: jorge.jovicich@unitn.it*

Background: The European Joint Programme on Neurodegenerative Disease Research (JPND) committed to our SRA-NED Working Group (http://www.sra-ned.org/) the survey of the international community for identifying (1) current barriers for a harmonized use of MRI/PET/EEG biomarkers of neurodegenerative diseases and (2) community driven solutions to overcome them. **Methods:** A 10-minute survey (both multiple choice and open questions) was developed to gather information from relevant communities